

Characterization of Slow-Light in a LIL-Fabricated Si₃N₄ Waveguide Grating

W.C.L. Hopman, D. Yudistira, R. Dekker, W.F.A. Engbers,

H.J.W.M. Hoekstra, R.M. de Ridder.

Mesa+ Research Institute, University of Twente,
P.O. Box 217, 7500 AE Enschede, The Netherlands

The paper presents results of a study of slow light excitation and power enhancement on a waveguide with a grated section. The 500 periods grating was successfully fabricated by combining a conventional mask lithography step with laser interference lithography. The grating was characterized using both an end-fire and an infrared camera setup to measure respectively the transmission and to map and quantify the power scattered out of the grating. We report an estimated factor for the group velocity slowdown in a finite periodic structure of about 10 times, corresponding to a speed of 0.1c.

Introduction

Slowing down the speed of light by an appreciable amount compared to its value in vacuum promises several interesting applications and phenomena like large time delays and field enhancement, e.g. for optical sensors, nonlinear optical devices, enhanced effective gain or low-threshold lasing [1-4]. Several mechanisms are known to provide a strongly reduced light velocity, like electromagnetically induced transparency [5], the coupled-resonator optical waveguide (CROW) [6], and photonic crystals [1].

Electromagnetic theory predicts a strongly reduced group velocity at the photonic band-edge of a medium with a periodically varying dielectric constant, e.g. a grating or another photonic crystal type. This so-called slow-light phenomenon which occurs when light with a free-space wavelength exactly at the photonic band edge is launched into the structure has been the subject of many studies [2,3,7,8,10,11].

In this work, we discuss slow light in a grating which was etched into a shallow silicon nitride (Si₃N₄) ridge waveguide (WG). We present a relatively simple method for estimating the intensity enhancement factor and hence the group velocity in the grating region by analyzing the light scattered from the structure. Using this method we show the group velocity at the photonic band edge of the grating to be an order of magnitude below the vacuum speed of light.

Design and Fabrication

In this section the design and fabrication scheme of the grated structures is presented. The fabrication started with LPCVD deposition of a 275 nm thick Si₃N₄ core layer on top of a 9 μm thick SiO₂ buffer layer, with a refractive index of respectively 1.981 and 1.445. Using conventional lithography, alignment markers were defined and etched into the Si₃N₄ layer. The ridge width is 7 μm satisfying the single mode condition, see figure 1 and 2. The 5 nm ridge was etched into the Si₃N₄ layer by use of the well controllable BHF wet-etching process. The used etch solution has a Si₃N₄-etch-rate of only ~0.7 nm/minute.

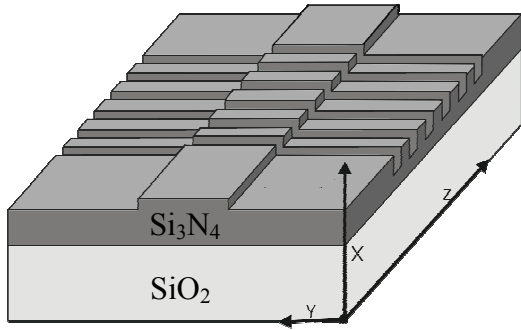


Fig 1: Schematic view of the 3D ridge-waveguide-grating, the polymer cladding is not drawn in this graph.

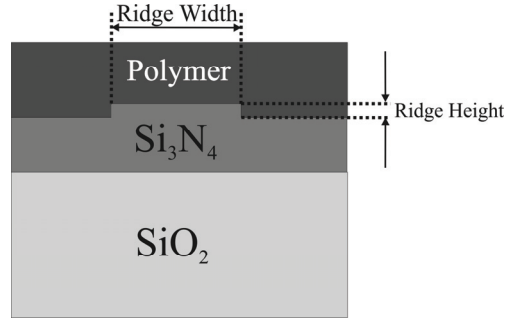


Fig 2: Schematic view of the ridge-waveguide and grating.

Next, a resist layer of approximately 400 nm suitable for image-reversal was spun unto the wafer. The 460 nm period gratings were defined using laser-interference lithography (LIL) [9], Lloyd's-mirror-setup, producing a pattern size of 2x4 cm. For many applications these dimensions exceed the limits posed by both the allowed chip-area and the scattering losses that are inherently present in highly perturbed subwavelength structures. Therefore, another mask was used to define the size (number of periods) of the gratings. A bright-field-type mask was chosen to protect the grating-regions for UV exposure. In the next step, the gratings were patterned using LIL. An image-reversal-bake was performed to make the exposed area inert to the developer solution. Multiple tests on this double exposure lithography step showed that a well-defined grating with 50% aspect ratio could be reproducibly obtained. A cross-section of the resulting resist pattern is shown in the inset of figure 3. The gratings were transferred to the Si_3N_4 -layer using RIE etching. Though the aimed etch depth of the gratings was 100nm, a slightly smaller etch depth of 60nm was estimated when the measurement data was fit using a mode expansion technique.

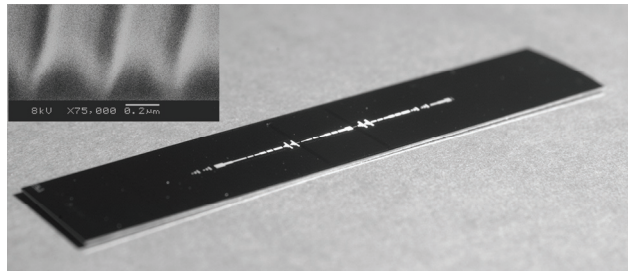


Fig 3: Photograph of the chip after dicing. The gratings are defined parallel to the long side of the chip. The various lengths (100 μm to 2.5mm) of the gratings are clearly visible. Top left corner: A SEM-photo of the resist obtained from the “double-exposure” tests.

Finally, after cleaning, the wafer was diced and the end faces were polished to make the sample suitable for characterization using end-fire coupling. Figure 3 shows a photograph of the chip that was used for the measurements. It clearly shows the multiple grating regions of different length which light up by diffraction of ambient light.

Characterization

The fabricated gratings were characterized using both an end-fire setup and an infrared sensitive camera. The camera was positioned to collect the scattering from selected area of the grating (see figure 4). A tunable laser (HP 8168c) was used as a light source and all measurements have been done with TE polarization. The measured normalized transmission spectrum is presented in figure 5. For the grating we find an on-off ratio as high as 20 dB, defined as the peak power at dielectric stop-band-edge (1544.2 nm) divided by the power measured in the stopband. The transmission curve shows sharp fringes, both on the larger and on the lower wavelength side of the stopband.

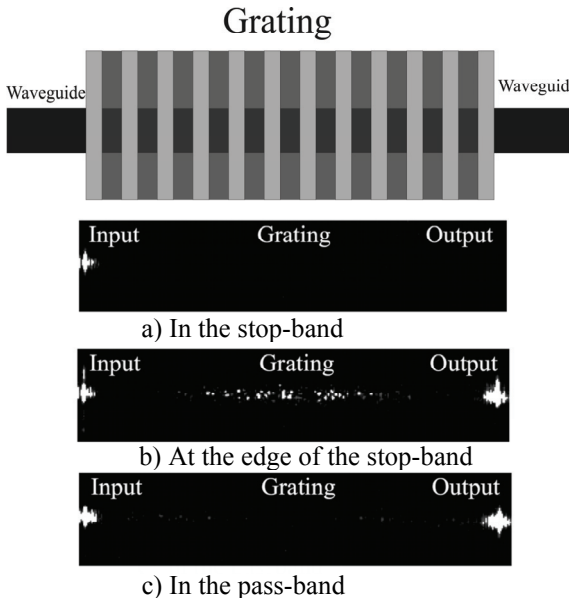


Fig 4: Three (cropped) camera shots of the device taken for wavelengths in the stopband, near the edge and outside the stopband (dielectric band). The top graph shows the position of the grating and in and output waveguides.

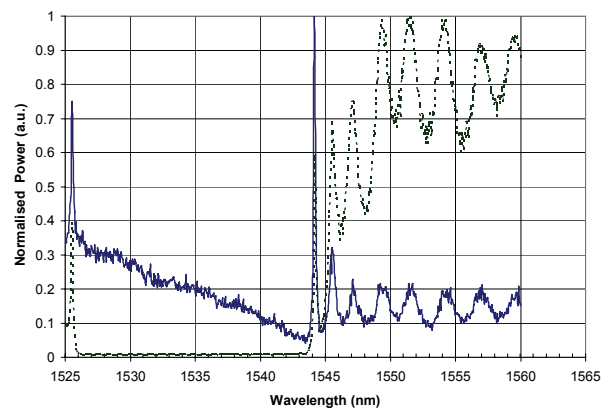


Fig 5: The normalized collected power scattered in the grating region (solid line) and the normalized transmission measured using an end-fire setup, versus the wavelength (dotted).

The available IR-camera produced images of 320x240 pixels, each pixel representing a $0.8 \mu\text{m} \times 0.8 \mu\text{m}$ chip areas. Figure 4 shows three camera frames taken at different wavelengths. The in and output facet of the grating can easily be distinguished by the relatively high scattering from these spots. The first resonant cavity mode right of the stop band is clearly recognizable for a wavelength of 1544.2 nm. Figure 5 shows also (solid line) the collected scatter light from the grating region as a function of the wavelength. The scatter-data show a sharp peak just above (and just below) the stopband of the grating. From the theory for 1-dimensional structures [10] we know the largest density of modes and lowest group-velocity is expected to occur in that wavelength region. It is not straightforward to calculate the power enhancement at the resonant wavelength, mainly because we only have the scattered power of the grating in resonance at that wavelength. To obtain a conservatively estimated figure for this enhancement we define this as peak intensity at 1544.2nm divided by the average intensity from 1543.7 to 1550.65nm. This leads to a power enhancement ratio of ~ 7 . It is assumed the group velocity slowdown is proportional to power enhancement [11]. Since the group velocity of the noncorrugated WG is about 1.5, we derive a minimum

for the measured group velocity in our structure of $\sim c/10 = 0.1c$. From figure 4 it is clear the out of plane scattering at the grating end facets is relatively high. Recent studies [2] propose that this impedance mismatch could be solved by introducing tapered sections as lead in and lead out. Etch-depth tapering could be a candidate for such a smooth transition, though this will require a more complicated fabrication scheme. Further studies on this type of slow-light device should make clear if these tapers can minimize the out-of-plane losses at the in and output of the grating while the same level of group velocity slowdown is maintained.

Conclusions

A WG grating has successfully been realized in Si_3N_4 using CMOS compatible technology by combining both conventional and laser interference lithography. The transmission spectrum of this device measured using an end-fire setup, showed an on-off ratio of ~ 20 dB. A strongly increased amount of Raleigh scattering was observed for a wavelength near the stop-band-edge in the grating region using an infrared sensitive camera. From this scattering data we have derived a number for the maximum achieved local power enhancement ratio. In this device we found an estimated factor of ~ 7 . Under assumption the group velocity is inverse proportional to this factor, we calculated a group velocity of $0.1c$. Further modeling is desired to verify the outcome of our measurements and to compare the “quality” of our devices with respect to inhomogenities to the ideal model.

References

- [1] E. Yablonovitch, "Inhibited spontaneous emission in solid-state physics and electronics", Phys. Rev. Lett., vol. 58, pp. 2059-2062, 1987.
- [2] M.L. Povinelli, S.G. Johnson, J.D. Joannopoulos, "Slow-light, band-edge waveguides for tunable time delays", Opt. Exp., vol. 13, pp. 7145-7159, 2005.
- [3] V.I. Kopp, B. Fan, H.K.M. Vithana, A.Z. Genack, "Low-threshold lasing at the edge of a photonic stop band in cholesteric liquid crystals", Opt. Lett., vol. 23, pp. 1707-1709, 1998.
- [4] W.C.L. Hopman, P. Pottier, D. Yudistira, J.V. Lith, P.V. Lambeck, R.M. De La Rue, A. Driessens, H.J.W.M. Hoekstra, R.M. de Ridder, "Quasi-one-dimensional photonic crystal as a compact building-block for refractometric optical sensors", IEEE Quant. Elect., vol. 11, pp. 11- 15, 2005
- [5] L.V. Hau, S.E. Harris, Z. Dutton, and C.H. Behroozi, "Light speed reduction to 17 meters per second in an ultracold atomic gas", Nature, vol. 397, pp. 594-598, 1999.
- [6] A. Yariv, Y. Xu, R.K. Lee, A. Scherer, "Coupled-resonator optical waveguide: a proposal and analysis", Opt. Lett., vol. 24, pp. 711-713, 1999.
- [7] D. Yudistira, H.J.W.M. Hoekstra, H. Hammer, D.A.I. Marpaung, "Slow light excitation in tapered 1D photonic crystals: theory", Opt. Quant. Elect. (Submitted 2005).
- [8] S. Johnson, M. Bienstman, M. Sakroboogatyi, H. Ibanescu, E. Lidorikis, J. Joannopoulos, "Adiabatic theorem and continuous coupled-mode theory for efficient taper transitions in photonic crystals", Phys. Rev. E., vol. 66, pp. 66608, 2002.
- [9] S. Vogelaar, W. Nijdam, H.A.G.M. van Wolferen, R.M. de Ridder, F.B. Segerink, E. Flück, L. Kuipers, N.F. van Hulst, "Large area photonic crystal slabs for visible light with wavelength defect structures: Fabrication with focuses ion beam assisted laser interference lithography", advanced materials, vol. 13, pp. 15511-15514, 2001.
- [10] J.M. Bendickson and J.P. Dowling, "Analytic expressions for the electromagnetic mode density in finite, one-dimensional, photonic band-gap structures", Phys. Rev. E, vol. 53, pp. 4107-4121, 1996.
- [11] K. Sakoda, "Enhanced light amplification due to group-velocity anomaly peculiar to two- and three-dimensional photonic crystals", Opt. Exp., vol. 4, pp. 167-176, 1999.